Supporting online material for

Differential DNase I Hypersensitivity Reveals Factor-dependent Chromatin Dynamics

Housheng Hansen He[§], Clifford A Meyer[§], Mei Wei Chen, V. Craig Jordan, Myles Brown[*], X. Shirley Liu[*]

[§] These authors contributed equally

[*] To whom correspondence should be addressed. Email: Myles_Brown@dfci.harvard.edu, xsliu@jimmy.harvard.edu

Supplemental Figures

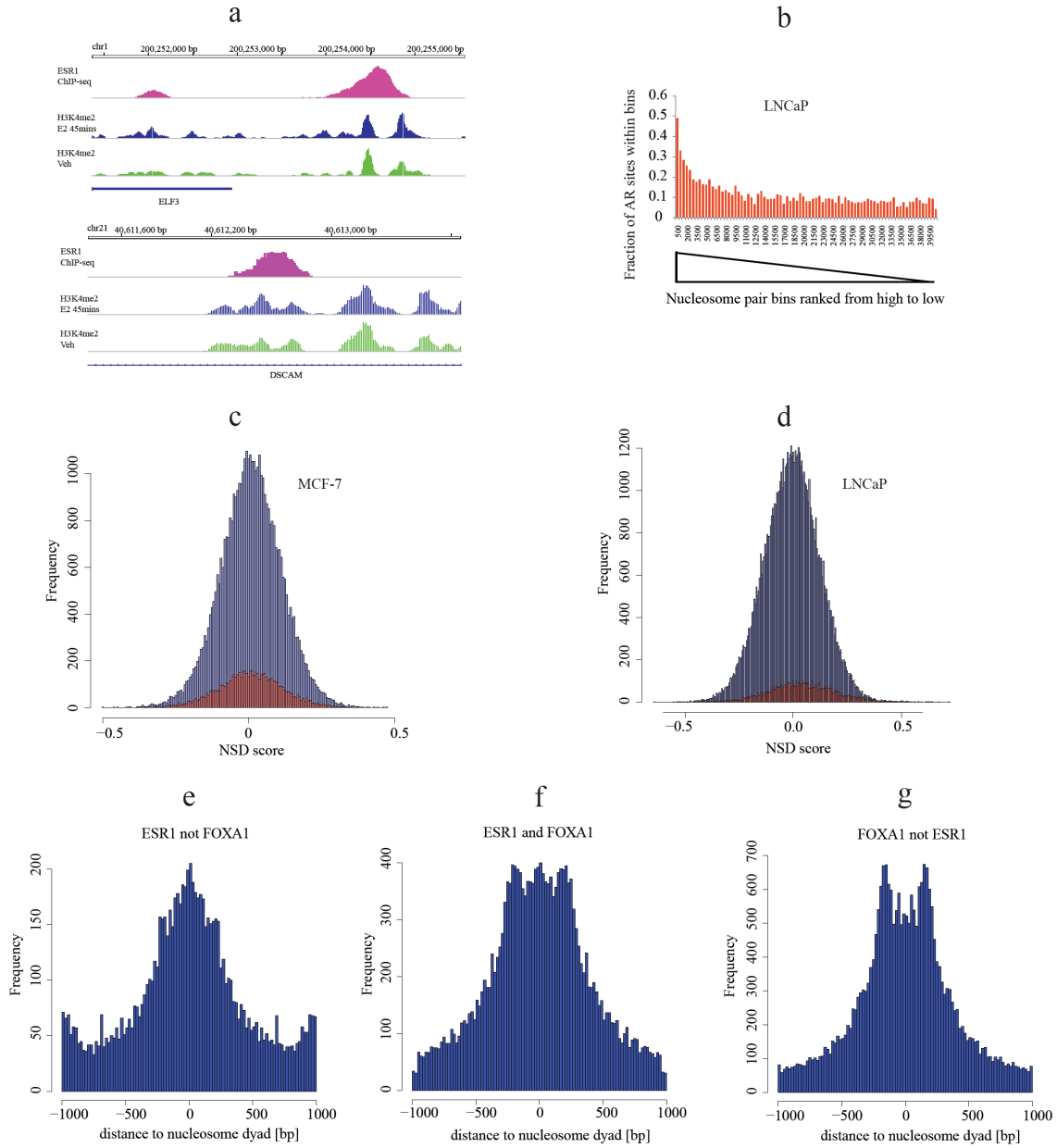

Supplemental Figure 1. ESR1 and AR binding and nucleosome occupancy. Instances of ESR1 binding located at depleted H3K4me2 regions near ESR1 regulated genes **(a)** ELF3 and DSCAM. **(b)** The fraction of AR binding sites in paired nucleosome bins sorted in descending order by NSD score (stimulated vs. unstimulated). Paired nucleosome regions are ranked by scores that represent the differences in the H3K4me2 tag counts before and after estrogen treatment. To calculate the proportion of real binding sites as a function of rank, these ranked regions are grouped into bins of 500. The y-axis represents the number of regions in each bin that overlap with AR ChIP-seq enriched regions. Distribution of NSD score of (**c**) non-ESR1 (blue) and ESR1 overlapping (red) paired nucleosome regions in MCF-7 and (**d**) non-AR (blue) and AR overlapping (blue) paired nucleosome regions (red) in LNCaP cells. Wilcoxon test was performed to analyze the differences between ER and non-ER (p-value = 0.25), AR and non-AR (p-value=2.2e-16) paired nucleosome regions. Distribution of the distance between **(e)** ESR1 unique **(f)** ESR1/FOXA1 shared and **(g)** FOXA1 unique binding sites and the nearest H3K4me2 marked nucleosomes. The x-axis represents the distance from the center of positioned nucleosomes as determined by the NPS software. The y-axis represents numbers of ESR1 or FOXA1 binding sites within given distance ranges.

a

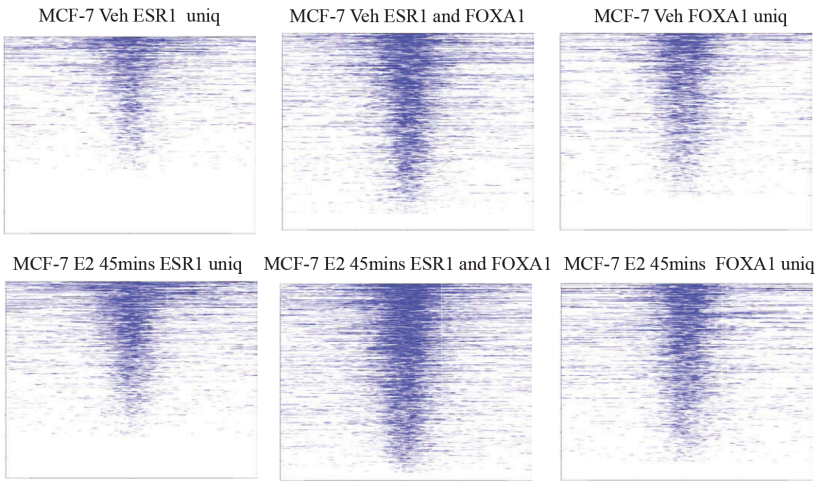
MCF-7 Veh ESR1 uniq
MCF-7 Veh ESR1 and FOXA1
MCF-7 Veh FOXA1 uniq
MCF-7 E2 45mins ESR1 uniq
MCF-7 E2 45mins ESR1 and FOXA1
MCF-7 E2 45mins FOXA1 uniq

b

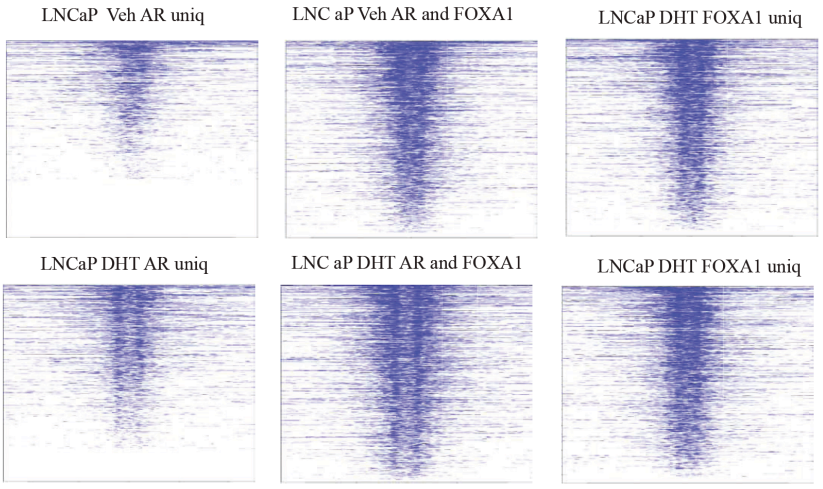
LNCaP Veh AR uniq
LNC aP Veh AR and FOXA1
LNCaP DHT FOXA1 uniq
LNCaP DHT AR uniq
LNC aP DHT AR and FOXA1
LNCaP DHT FOXA1 uniq

c

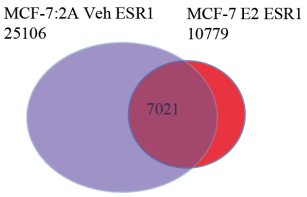
MCF-7:2A Veh ESR1
25106
MCF-7 E2 ESR1
10779
7021

d

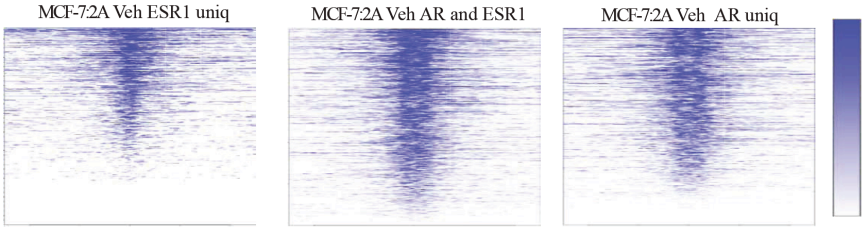
MCF-7:2A Veh ESR1 uniq
MCF-7:2A Veh AR and ESR1
MCF-7:2A Veh AR uniq

Supplemental Figure 2. Mono-nucleosome level H3K4me2 ChIP-seq at nuclear receptor and FOXA1 binding loci in the (a) MCF-7, (b) LNCaP and (c), (d) MCF-7:2A cell lines. (a) Top panel, the distribution of H3K4me2 signal centered on AR-unique, AR/FOXA1 shared and FOXA1-unique sites in the unstimulated condition. Bottom panel, distribution of H3K4me2 signal centered on the AR-unique, AR/FOXA1 shared and FOXA1-unique sites under conditions of androgen stimulation. (b) Top panel, distribution of H3K4me2 signal centered on ESR1-unique, ESR1/FOXA1 shared and FOXA1-unique sites in unstimulated cells. Bottom panel, distribution of H3K4me2 signal centered on ESR1-unique, ESR1/FOXA1 shared and FOXA1-unique sites in estrogen stimulated cells. (c) Venn diagram of MCF-7 ESR1 binding in relation to MCF-7:2A ESR1 binding. (d) Distribution of H3K4me2 signal centered on ESR1-unique, ESR1/AR shared and AR-unique sites in unstimulated cells.

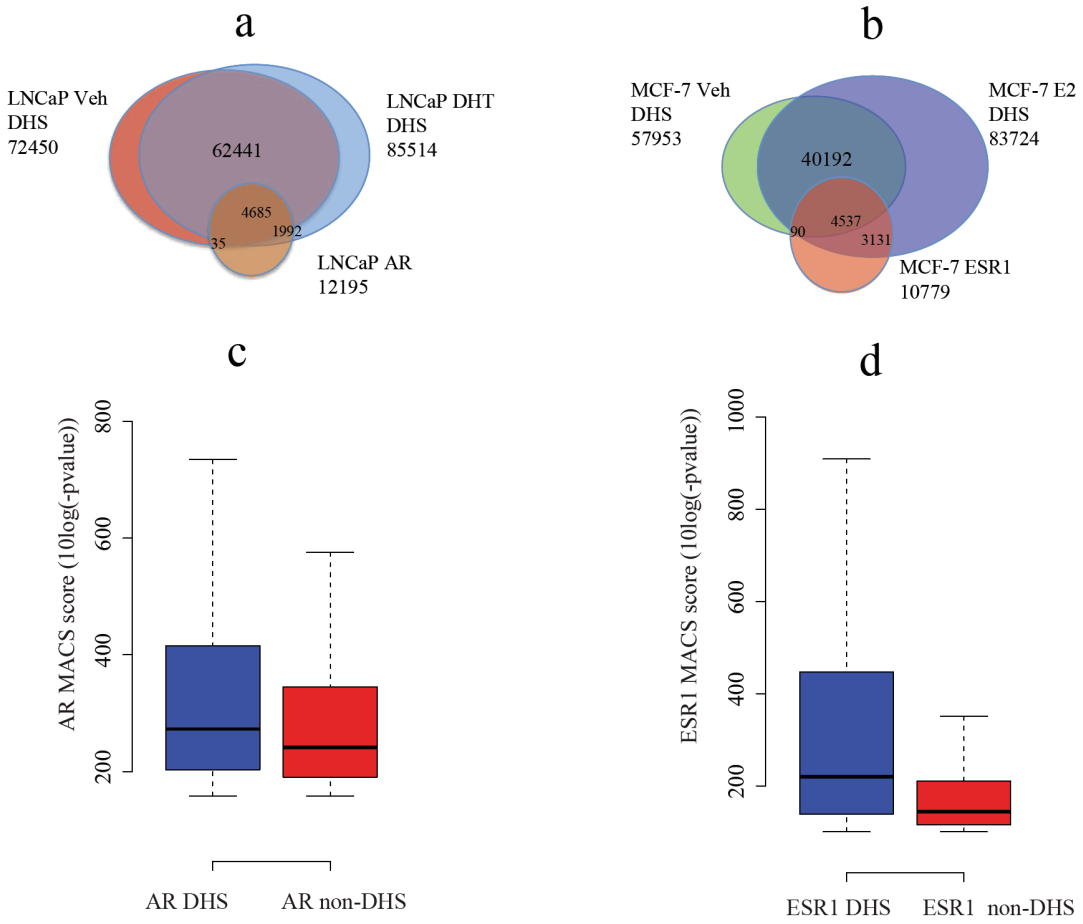

Supplemental Figure 3. DNase I hypersensitivity sequencing in LNCaP and MCF-7. **(a)** Venn diagram of DHS and AR peaks in LNCaP. DHS was identified at the sequencing depth of 50M for un-stimulated and 70M for androgen stimulated conditions. **(b)** Venn diagram of DHS and ESR1 peaks in MCF-7. DHS was identified at the sequencing depth of 28M for un-stimulated and 70M for estrogen stimulated conditions. **(c)** AR and **(d)** ESR1 binding level is measured by MACS p-value (-10log(p-value)). "AR DHS" and "ESR1 DHS" represent the respective AR and ESR1 binding sites

overlapping with DHS; “AR non-DHS” and “ESR1 non-DHS” represent the AR and ESR1 binding sites not overlapping with DHS.

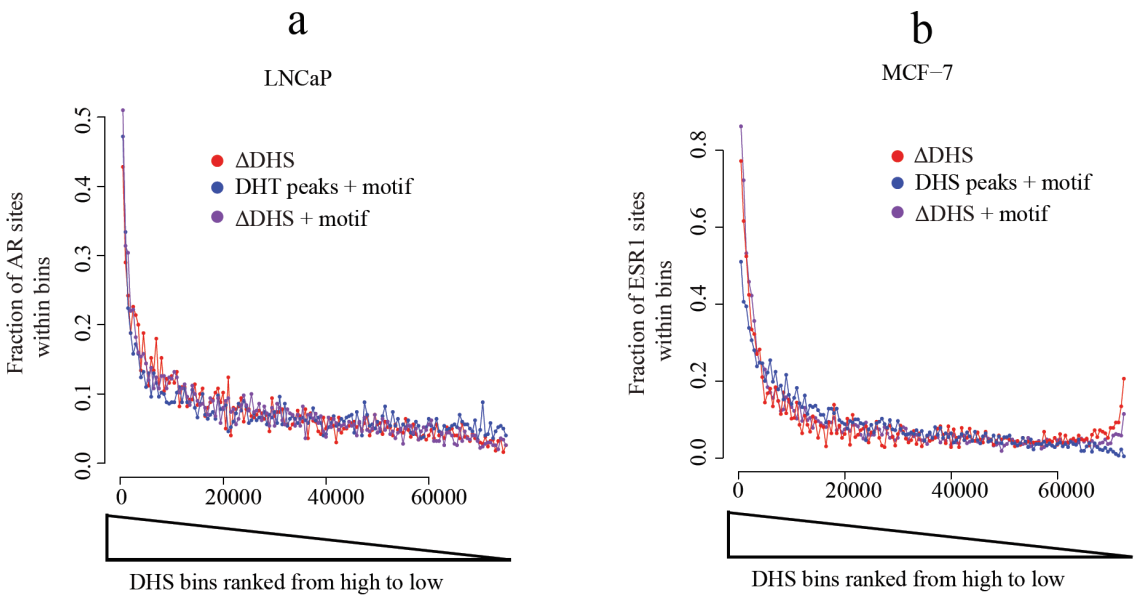

Supplemental Figure 4. Characteristics of DNaseI hypersensitivity sequencing. The fraction of **(a)** LNCaP AR and **(b)** MCF-7 ESR1 binding sites in bins of 500 DHS sites ranked by three measures: ΔDHS, the change in DNAseI hypersensitivity between conditions, respective AR and ESR1 motifs in LNCaP and MCF-7 DHS under hormone stimulated conditions, and the combination of the two measures. For the combination of ΔDHS and motif, the formula sqrt((ΔDHS rank)*(motif rank)) was used. The regions are ranked by the respective statistics before grouping into bins of 500. The y-axis represents the number of regions in each bin that overlap with **(a)** AR and **(b)** ESR1 ChIP-seq enriched regions.

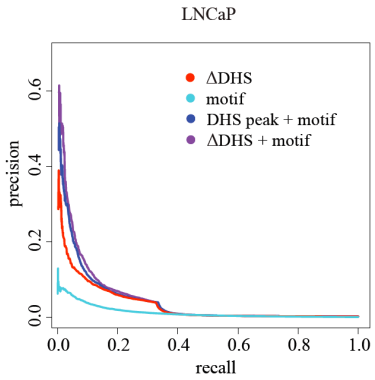

Supplemental Figure 5. Precision-recall analysis of prediction power using DNase I hypersensitivity sequencing. The precision-recall curves for prediction power of LNCaP AR binding sites were calculated by four measures: ΔDHS, AR motif rank, AR motif in DHT DHS and sqrt((ΔDHS rank)*(motif rank)).

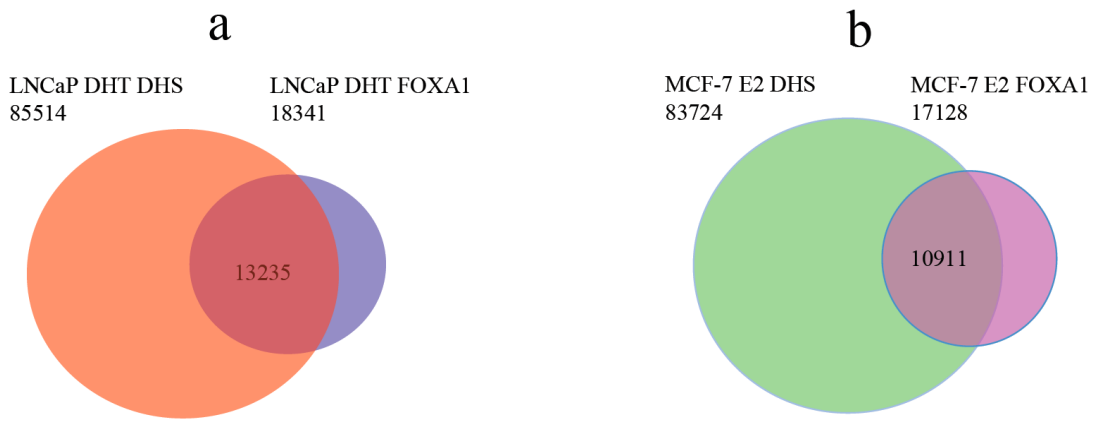

Supplemental Figure 6. Overlap between DHS and FOXA1 in (a) LNCaP (b) and MCF-7. MACS peak regions under hormone-stimulated conditions were used for comparison.

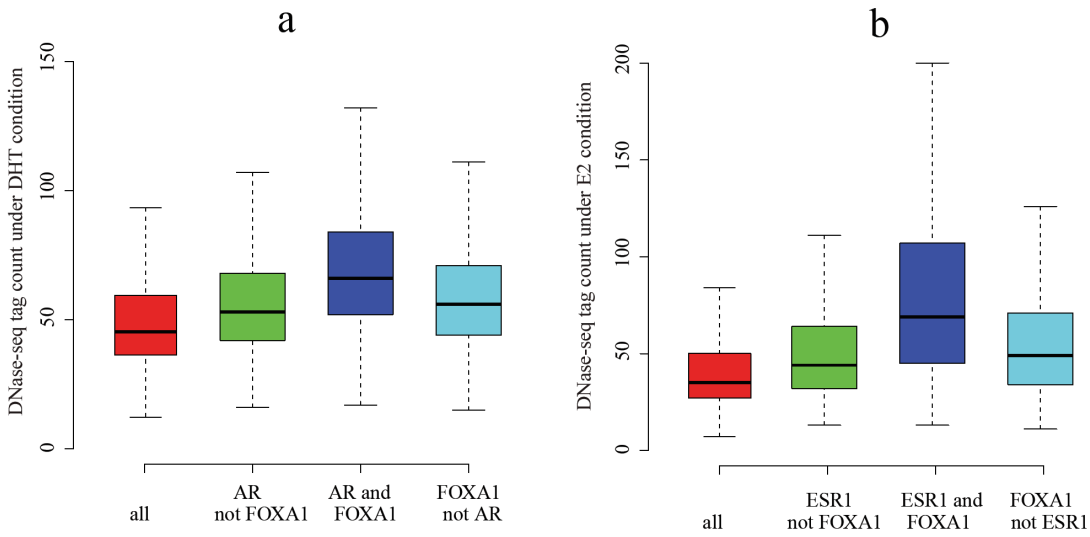

Supplemental Figure 7. DNaseI-seq signal of (a) AR and FOXA1 and (b) ESR1 and FOXA1 subsets under hormone stimulated conditions. "all" represents all the DHS sites in MCF-7 and LNCaP; "AR not FOXA1" and "ESR1 not FOXA1" represent AR and ESR1 binding sites that do not overlap with FOXA1; "AR and FOXA1" and "ESR1 and FOXA1" represent AR and ESR1 binding sites that overlap with FOXA1; "FOXA1 not AR" and "FOXA1 not ESR1" represents FOXA1 binding sites that do not overlap with AR and ESR1.

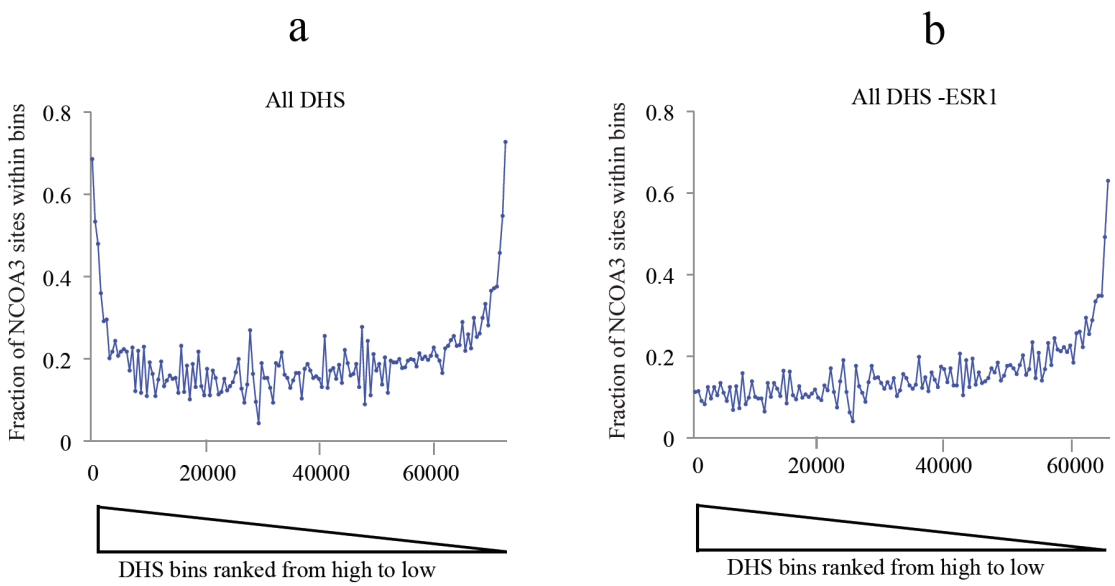

Supplemental Figure 8. DNase I hypersensitivity changes at NCOA3 sites. Association of ΔDHS with NCOA3 sites in the presence (a) and absence (b) of ESR1 binding. MCF-7 DHS sites under the stimulated condition were ranked by decreasing ΔDHS score. These ranked regions are grouped into bins of 500. The y-axis represents the fraction of regions that overlap with NCOA3 ChIP-seq enriched regions.

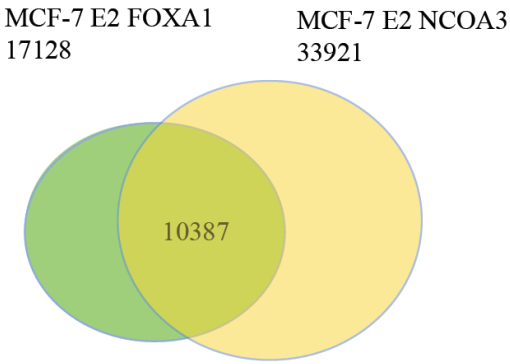

Supplemental Figure 9. Overlap between FOXA1 and NCOA3 in MCF-7. MACS peak regions under hormone-stimulated conditions were used for comparison. Venn diagram shows that 10387 out of the 17128 (61%) FOXA1 binding sites overlap with NCOA3 binding.

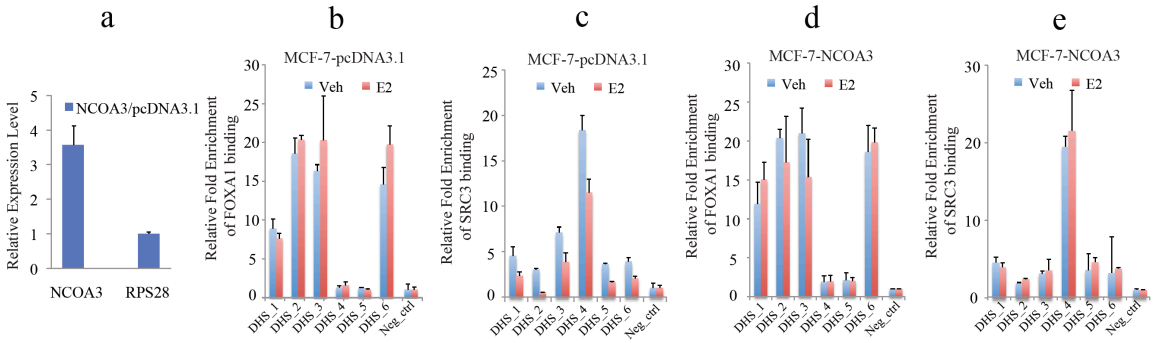

Supplemental Figure 10. Overexpression of NCOA3 in MCF-7. (a) RT-qPCR shows that the NCOA3 level in the NCOA3 overexpression sample is 3.5 fold higher than in the control sample which was transfected with empty pcDNA3.1 vector. The housekeeping gene RPS28 is used as an internal control. ChIP-qPCR of (b) FOXA1 and (c) NCOA3 in MCF-7 cells transfected with an empty pcDNA3.1 vector. ChIP-qPCR of (d) FOXA1 and (c) NCOA3 in MCF-7 cells transfected with an NCOA3 overexpression plasmid.

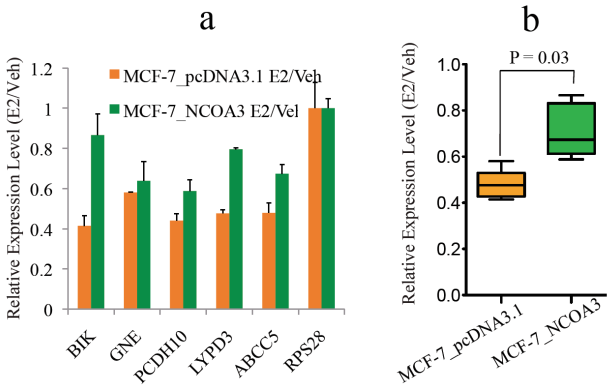

Supplemental Figure 11. The effect of NCOA3 overexpression on estrogen down-regulated genes. (a) Five genes that are down-regulated after 40 mins of estrogen stimulation (GRO-Seq data) were selected. RT-qPCR shows the fold changes of target gene expression after estrogen stimulation for 3 hours in the MCF-7 cells transfected with control plasmid and NCOA3 overexpression plasmid. (b). Box plots generated from RT-qPCR data of the 5 genes tested in (a). Overexpression of NCOA3 diminished the estrogen-induced down-regulation of target genes.

Supplemental Table 1. Primers used for PCR.

Primers used in Supplemental Figure 10

NCOA3_exp_F	GAATCCCATGATGCAACACC	NCOA3_exp_R	GCCATTCATGTGCACCATAC
DHS_1_F	CTTAGCCCAAAGCACCCAAT	DHS_1_R	CACTCCAGCCTGGGCAAC
DHS_2_F	GGCTGTCTGCATCCTCTCAC	DHS_2_R	CCAGCACCTTGGGTAAACAG
DHS_3_F	AAACCTGCCAAGTCAGAAGC	DHS_3_R	CAGAGACAGCAAGAGAGAGAGA
DHS_4_F	GAAGTTTATTTGCCATCACAGGT	DHS_4_R	TTCCTGGACATCCTGTGAAAC
DHS_5_F	AGGGAACCATGATTGACAGC	DHS_5_R	TGGGTCACTAATTGAAGAAAAATG

DHS_6_F	ACTCCACGAGCCCTGATTTT	DHS_6_R	GCTTCTATTGGTGGACAAGCA
DHS_7_F	CAACACCTTCCTGGTCCAGATAC	DHS_7_R	AAGGGAAACAGAGATCATCTGGAGT
Neg_ctrl_F	TCAGCTTTGACTGCCACCTA	Neg_ctrl_R	GGACATTTTCCTCCTGGTTCT
Primers used in Supplemental Figure 11			
BIK_exp_F	CTGCATCGGGGACGAGAT	BIK_exp_R	AGTGTGGTGAAACCGTCCAT
GNE_exp_F	ATCTCATCCAAGCTGCGAAA	GNE_exp_R	GATCACAAGGGAGGGATTCA
PCDH10_exp_F	TACGGACACTGAGCACAACC	PCDH10_exp_R	CTGTTAACTCGGCGAGGTCT
LYPD3_exp_F	ACAAGATGAAGACAGTGAAGTGC	LYPD3_exp_R	GAAGCCCGTGAAGATCCAG
ABCC5_exp_F	ACTTCTCAGTGGGGGAACG	ABCC5_exp_R	CAGTCTGCAAATGCTTCTCG
RPS28_exp_F	CGATCCATCATCCGCAATG	RPS28_exp_R	AGCCAAGCTCAGCGCAAC